

Density and capture radius of 'defects': quenching of the luminescent states in non-nitrogenated and nitrogenated amorphous carbon thin films

This article has been downloaded from IOPscience. Please scroll down to see the full text article.

2002 J. Phys.: Condens. Matter 14 13231

(<http://iopscience.iop.org/0953-8984/14/48/373>)

View [the table of contents for this issue](#), or go to the [journal homepage](#) for more

Download details:

IP Address: 171.66.16.97

The article was downloaded on 18/05/2010 at 19:17

Please note that [terms and conditions apply](#).

# Density and capture radius of ‘defects’: quenching of the luminescent states in non-nitrogenated and nitrogenated amorphous carbon thin films

G Fanchini<sup>1</sup>, S C Ray<sup>1</sup>, A Tagliaferro<sup>1</sup> and E Laurenti<sup>2</sup>

<sup>1</sup> Dipartimento di Fisica & Unità INFN, Politecnico di Torino, Torino, Italy

<sup>2</sup> Dipartimento di Chimica IFM, Università di Torino, Torino, Italy

E-mail: fanchini@polito.it

Received 27 September 2002

Published 22 November 2002

Online at [stacks.iop.org/JPhysCM/14/13231](http://stacks.iop.org/JPhysCM/14/13231)

## Abstract

The properties of photoluminescence (PL) in nitrogenated and non-nitrogenated amorphous carbon films are discussed. Emphasis is given to nitrogenated films and their peculiarities. The role of oxygen, through structural relaxation, and of nitrogen, due to structural relaxation and lone pairs, is discussed. A general correlation between the density of diamagnetic and paramagnetic ‘defects’ of different extensions and the quantum efficiency of PL is found. It is also shown that a-CN films can be divided in two categories, following their local structure and, in particular, the presence of voids, that lead to large scale oxygen contamination and stress release.

## 1. Introduction

Amorphous carbon-based thin films are rather peculiar due to the coexistence, in their microstructures, of  $sp^3$  (tetrahedral, diamond-like) and  $sp^2$  (hexagonal, graphite-like) hybridized carbon sites. Their relative amounts can be varied depending on the preparation conditions, tailoring the film properties. The  $sp^2$  sites tend to form clusters of different shapes and sizes, where localized  $\pi$  electrons are confined and paramagnetic and non-paramagnetic ‘defects’ of controversial nature are embedded in concentrations (from  $10^{17}$  up to  $10^{21}$   $\text{cm}^{-3}$ ) dependent on the film properties [1].

Nitrogen addition in amorphous carbons introduces further degrees of freedom in the film properties, involving the appearance of  $sp^1$  carbon sites [2].  $sp^2$  carbon sites involve three (strongly bonded)  $\sigma$  electrons and one (more weakly bonded)  $\pi$  electron each. Each  $sp^1$  carbon site involves two  $\sigma$  electrons and two  $\pi$  electrons, resulting in a higher number of weakly bonded electrons. Furthermore, also nitrogen may exhibit different hybridizations [3–8].

A key point is that nitrogen, when incorporated in nitrile groups and, more generally, in most groups involving  $sp^1$  carbon and nitrogen (but also in ‘pyridine-like’ rings [2], if this happens), involves two lone-pair (LP) electrons per atom. An important concentration of LP

**Table 1.** Deposition conditions and main features of the samples.

	Ar	$N_2$	Pressure	rf power	$V_b$	$D_{el}$	N	$E_{gap}$	$N_d$ $N_p$		Para-	References
	flux	flux							$(10^{20} \text{ cm}^{-3})$			
	(sccm)	(sccm)	(mTorr)	(W)	(V)	(mm)	(%)	(eV)				
A	50	20	20	300	880	15	30	0.36	3	3	Pauli	[5, 20]
B	70	20	20	150	570	15	30	1.30	1	4	Curie	[5, 20]
											(>7 K)	
C	70	20	20	300	980	15	27	0.35	3	5	Pauli	[5, 20]
D0	0	80	15	150	570	15	10	1.25	1	0.1	Curie	[20, 21]
D1	0	80	15	150	700	20	10	1.20	0.7	0.1	Curie	[20, 21]
D2	0	80	15	150	730	25	10	1.15	0.4	0.1	Curie	[20, 21]

electrons is then present, for instance, in a carbon nitride thin film with 30 at.% of nitrogen and the DOS is therefore that shown in figure 1.

Another relevant issue of the nitrogen incorporation is the strong photoluminescence (PL) enhancement exhibited by floppy, low gap ( $<1.5$  eV) amorphous carbon nitride (a-CN) based thin films [13–15], while, for instance, polymer-like hydrogenated amorphous carbons (a-C:H) exhibit similar PL efficiencies only [14] with high hydrogen contents ( $>50\%$ ), wider gaps ( $>3$  eV) and high resistivity. In this work, the analysis of several (vibrational, optical, paramagnetic) properties of a set of a-CN thin films will be applied to the study of their PL behaviour.

## 2. Experimental details

The films detailed in the present work are representative of a larger set of films. They were prepared onto (100) c-Si and glass substrates by radio-frequency (13.56 MHz) sputtering a graphite target (99.999% purity) in nitrogen or argon/nitrogen atmospheres. In all cases no deliberate substrate biasing was applied. Two series of samples were examined. Since previous experiments with the same [16] or similar [17] deposition systems have shown that the most relevant parameters controlling the growth were the nitrogen partial pressure ( $p_N$ ) and the system self-bias voltage ( $V_b$ ), four samples (A, B, C, D0) grown at  $p_N$  ranging from 5.7 to 15 mTorr and  $V_b$  ranging from 570 to 980 V are considered. In the framework of this set, only one relevant parameter was changed from one deposition to another: for instance, samples A and C were grown by changing  $p_N$  through a change of the argon flow rate, at constant power and total chamber pressure (i.e. at a quasi-constant  $V_b$  value); samples B and C were grown by changing the microwave power (and, subsequently, by relevantly changing the self-bias voltage) by a factor  $\sim 2$  at a constant  $p_N = 5.7$  mTorr. Samples B and D0 were grown at the same bias voltage ( $V_b = 570$  V) which has been reached, at a constant radio-frequency power, by a simultaneous change of the total pressure and the gas fluxes. Since, as shown below, sample D0 is the most luminescent of these series, its deposition conditions have been exploited by enlarging, at constant power, pressure and gas flux, the distance between the electrodes  $D_{el}$ . Different films (D0, . . . , D2) were obtained at different electrode spacings. The deposition conditions are indicated in table 1, also reported are some references to other works where the same (or similar) samples are characterized. C-type samples are A and C.

## 3. Results and discussion

Recently, we observed [20] that our reactive-sputtered a-CN thin films can be roughly divided in two categories, depending on their microstructure.

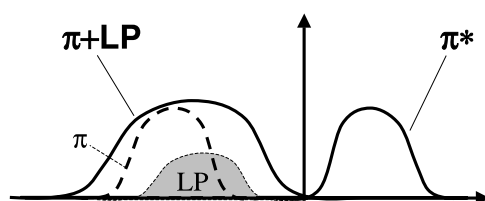


**Figure 1.** Sketch of the density of electronic states (DOS) in disordered carbon nitrides.

**Table 2.** Features distinguishing B- and C-type samples.

Feature	B-type	C-type
Tauc gap (at a given N content)	Higher	Lower
CN peak @ $\sim 2200 \text{ cm}^{-1}$	Upshifted composite	Downshifted single feature
OH inclusions (figure 2)	Present	Absent
$N_{SB}/N_{CN}$ (figure 3)	50	22
Paramagnetism	Curie ( $\propto T^{-1}$ )	Pauli
PL efficiency	Higher	Lower
Recombination (see equation (2))	$\alpha > 1$ (except sample B)	$\alpha < 1$

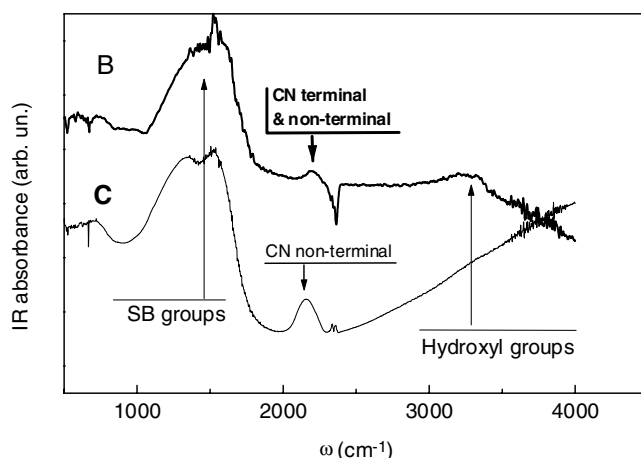
- (i) Soft and ‘bubbly’ (B-type) a-CN films with optical gap of 1–1.5 eV and floppy microstructures with high PL background but poor transport properties.
- (ii) More connective a-CN films with lower gaps and higher internal stresses exhibiting lower PL background, but a more graphite-like, conductive character. With our sputtering system, C-type samples grow at lower rf powers and higher total pressures, by keeping the other conditions fixed, otherwise leading to B-type films [20].

It is stressed that such a classification is quite independent of the nitrogen content as we can anticipate that a-CN thin films with similar nitrogen contents may fit the two different categories (see for instance films A and B both presenting N content of 30% as measured by RBS). In table 2 some characteristics differentiating the two categories are indicated.

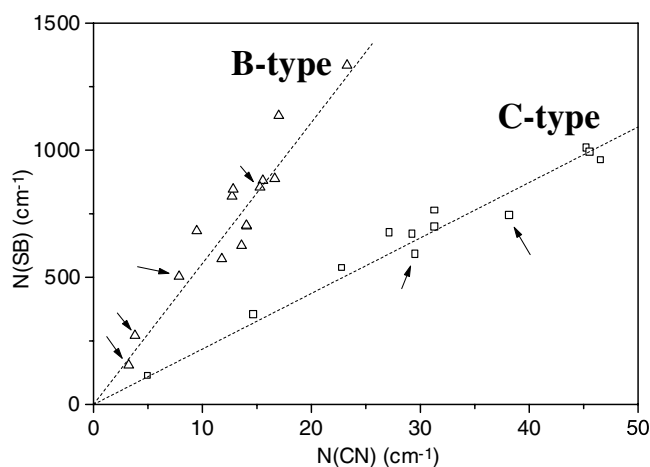
### 3.1. IR characteristics

Figure 2 presents two overall FTIR spectra of a B-type and a C-type sample. Several IR features are able to distinguish B- and C-type a-CN films. They are detailed in [20]. Here we mention the following.

- (1) The intensity of the OH stretching contributions (O–H, O–H  $\cdots$  N, O–H  $\cdots$  O, ...) around  $3500 \text{ cm}^{-1}$  [23]. It may be observed that B-type films present huge hydroxyl contributions, while such contributions are absent in C-type films. Since O and H were not purposefully introduced in the deposition chamber, such contributions are formed due to the atmospheric exposure of the films. Being related to the diffusivity of the atmospheric water vapour the OH peaks are good indicators [3] of the softness and the porosity of the B-type films.
- (2) The shape and position (figure 2, detail) of the CN peaks. It has been shown that B-type films presenting terminal nitrile groups or mixtures of terminal and non-terminal groups have more composite CN peaks with maxima at higher frequency positions ( $2200 \text{ cm}^{-1}$  or above [24]). C-type films owe part of their compactness to the predominance of



**Figure 2.** FTIR spectra of a B-type and a C-type sample. The main regions of interest (see text) are indicated. The differences in shape at  $\sim 2200\text{ cm}^{-1}$  (single-Gaussian or composite) and peak values are due to the different vibrating groups (terminal + non-terminal in B-type samples, or only non-terminal in C-type ones). The flat region at  $\sim 3300\text{ cm}^{-1}$  in the C-type sample (i.e. the absence of OH) is an indicator of its compactness.



**Figure 3.** Relationship between the (total) optical oscillator strength densities in the  $1000\text{--}1900\text{ cm}^{-1}$  (SB) and  $\sim 2200\text{ cm}^{-1}$  (CN) regions. It is different for B- and C-type samples. The arrows indicate the samples considered in the present work.

non-terminal groups (possibly carbodimide-like chains) stretching at lower frequencies (i.e.  $2150\text{ cm}^{-1}$  or lower [24]).

- (3) The optical strength densities of the SB peaks at  $1000\text{--}1900\text{ cm}^{-1}$   $N_{SB}$  are proportional to the optical strength density of the CN peaks  $N_{CN}$  (figure 3). The origin of such a proportionality was indicated in the polarization effects that the nitrogenated inclusions operate on the back-bonded  $sp^2$  carbon phase [4]. Different proportionality trends were found for B- and C-type samples, as a consequence of the different (non-terminal and mainly—but not only—terminal) nature of the CN groups involved by the two classes of films.

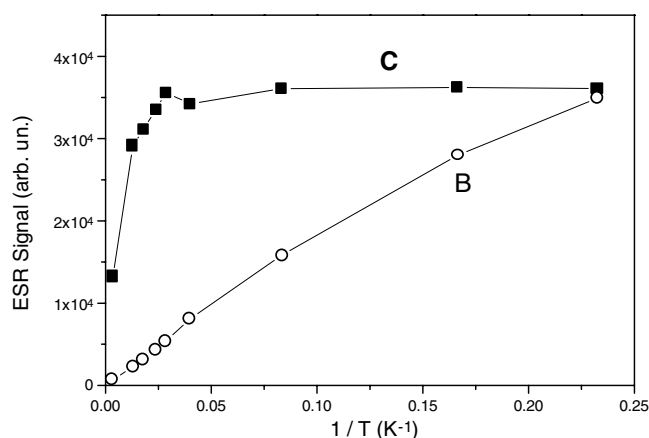


**Figure 4.** Different forms of paramagnetism in B- and C-type samples demonstrated by the different temperature trends of the intensity of the ESR signal.

Several examples of FTIR spectra of samples presenting B-type (see for instance [17, 25, 26]) or C-type (see for instance [9, 16]) characteristics can be found in the literature.

### 3.2. Optical properties

In N-free amorphous carbons, the optical ( $T_{auc}$ ) gap does not have a well defined physical meaning related to a mobility edge, but it is just a conventional parameter [11]. In nitrogenated carbons, the LP electrons are supposed to play a role in determining the gap but the situation is not dissimilar. In general, lower gaps are related to higher delocalization of the  $\pi$  electrons.

C-type films present very low ( $T_{auc}$ ) gaps (in most cases 0.2–0.5 eV), to be compared with the wider gap (above 1 eV) exhibited by B-type samples. This is consistent with the prevalence, in C-type samples, of non-terminal CN groups, of which the  $\pi$  electrons (as discussed in [5]) may act as 'crosslinks' between the  $sp^2$  clusters providing a continuous network along the film. Things run differently in B-type samples where a large fraction of the CN groups, being terminal, improve the  $\pi$ -electron confinement in the  $sp^2$  phase which they are back-bonded to.

### 3.3. Paramagnetism

With respect to their paramagnetism, two different behaviours were found (see [5], figure 4).

- (1) B-type a-CN samples are semiconducting; they exhibit Curie-like paramagnetism (i.e. ESR signal proportional to  $T^{-1}$ ) and spin mobility occurring by hopping.
- (2) C-type a-CN samples exhibit Pauli-like paramagnetism (i.e. ESR signal constant with temperature, typical of semimetals). The semiconducting–semimetallic transition has been observed between 77 and 295 K.

This confirms the observations made on the basis of FTIR and optical measurements indicating more continuous and delocalized electronic structures for C-type films.

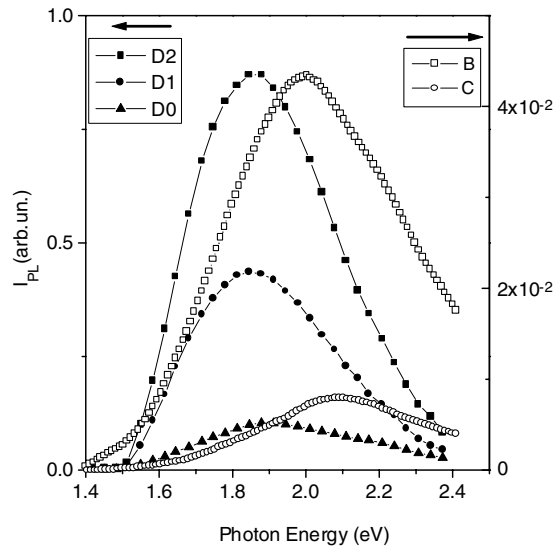


**Figure 5.** Room temperature PL spectra of the samples recorded at 2.4 eV excitation and a laser power of 50 mW on a spot size of  $3 \mu\text{m}^2$ .

## 4. Defects and luminescence

### 4.1. The recombination phenomena

The considered a-CN samples exhibit very different PL efficiencies, as can be seen in figure 5. In amorphous carbons, though stress release and low coordination number are generally assessed as necessary conditions to enhance the PL efficiency and quench the non-radiative recombination centres (see for instance [28, 29]), the details are much more difficult to understand than in mono-phase amorphous semiconductors (such as hydrogenated amorphous silicon, a-Si:H, where the defects—dangling bonds—are strongly localized) and similar difficulties are found in explaining the recombination processes in our samples. In mono-phase amorphous semiconductors, the quantum efficiency  $Y_0$  of the hole-pair creation process is assumed to be a material property, while the PL efficiency ( $Y < Y_0$ ) depends on the defect density (assumed, in a-Si:H, to coincide with the spin density  $N_s$  and to be due to homogeneously distributed centres) and on the non-radiative capture radius  $R_C$  related to the defect size [30]:

$$Y = Y_0 \exp[-4\pi R_C^3 N_s / 3]. \quad (1)$$

In amorphous carbons, the non-radiative recombination centres are not necessarily paramagnetic (i.e. ESR active) centres involving non-bonding electrons, but possibly also diamagnetic centres involving distorted bonding ( $\pi$ ) and antibonding ( $\pi^*$ ) states must be considered [29].

In a-CN, diamagnetic recombination centres are also represented by the LP electrons involved by most of the hypothesized forms of nitrogen incorporation. In summary, multiple effects on the PL processes may be associated with nitrogen.

- (1) If nitrogen is incorporated as terminal, nitrile, groups (or, more generally, as low-coordinated groups) it is accompanied by a strong release of the internal stresses, resulting in an enhancement of the PL.

- (2) In contrast, the LP electrons involved by nitrogen may act as non-radiative recombination centres, reducing the PL intensity.
- (3) However, especially in the presence of relevant amounts of disorder, the LP electrons tend to form ‘weak bonds’ with the surrounding ions (see section 1), resulting in an LP– $\pi$  mixing and the formation of ‘spurious’ bonding and antibonding states, where electron–hole pairs can sit.

Whereas ‘weak bonds’ are formed, the effects described in point (2) are not so important and the simultaneous occurrence of conditions (1) and (3) may explain the strong PL in low gap a-CN and a-CN:H, with respect to polymer-like hydrogenated amorphous carbons (a-C:H) exhibiting similar PL efficiencies only with high hydrogen contents.

Qualitative information on the capture radii  $R_C$  can be obtained by measuring the PL efficiency at different powers  $P$  of the excitation source and looking at the resulting trend, which, as a first-order approximation, can be described by the equation

$$Y(P) = K P^\alpha. \quad (2)$$

A detailed description of the processes involved by the different values of the exponent  $\alpha$  can be found in [30, 33]. These can be summarized observing the following.

- (1)  $\alpha > 0$  means that higher densities of electron–hole pairs (i.e. pairs closer to each other) increase the amount of radiative recombination, due to an increasing importance, at decreasing pair-to-pair distance, of non-geminate (multi-pair) recombination. Obviously, if this occurs, non-geminate processes are a relevant fraction of the luminescent processes.
- (2)  $\alpha = 0$  means that the PL intensity is independent of the pair-to-pair distance. This happens when each electron–hole pair recombination is independent of the others, occurring geminately.
- (3)  $\alpha < 0$  means that recombination occurs by the assistance of some kind of centre (typically defects) for which the abundance is of the order of that of the electron–hole pairs, so that producing larger numbers of pairs by increasing the excitation power results in a saturation of the radiative recombination processes. This usually happens when radiative recombination occurs by means of ‘Auger-like’ processes (i.e. a non-bonded electron moves deeper in the valence band saturating the hole) in concurrence with non-radiative processes induced by the defect.

#### 4.2. Recombination in ‘B-type’ a-CN(:OH)

The B-type a-CN films, being weakly or under-constrained, are often sensible to laser soaking effects, so that a reliable study of their luminescence behaviour versus power can be conducted ruling out possible microstructural modifications only after a prolonged laser soaking (e.g. 12 min at 50 mW of green light on a spot size of  $3 \mu\text{m}^2$  [21]). However, both before and after light soaking (figure 6), in the B-type samples D0, . . . , D2 the PL efficiency increases with power following equation (2) with  $\alpha > 0$ . Such an effect points to the relevance of non-geminate recombination, consistent with the microstructural properties of the films.

Beside the recombination processes, the PL mechanism in B-type a-CN(:OH) films seems to be quite similar to that currently observed in non-nitrogenated a-C:H (figure 7). Following Giorgis *et al* [29] equation (1) can be applied to all types of a-C:H, even polymer-like or diamond-like, if the total number of ‘defects’ acting as non-radiative centres is given by the sum of weakly optically active paramagnetic defects ( $N_p$ ) and optically active diamagnetic defects ( $N_d$ )

$$N_s = N_p + N_d(E < U). \quad (3)$$



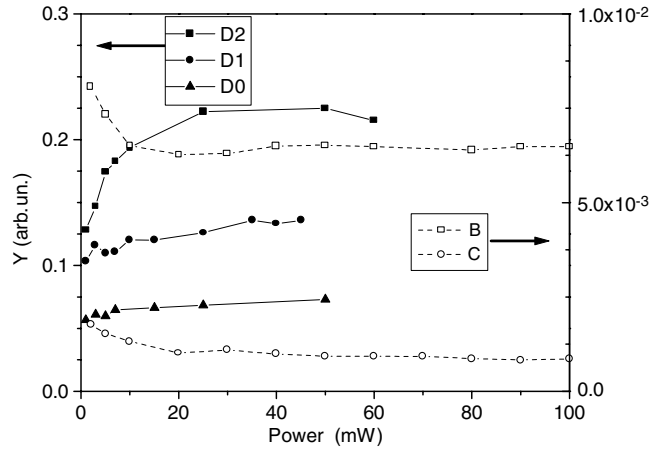


**Figure 6.** PL efficiency (integrated PL intensity divided by the power of the laser source) of the detailed samples (from data recorded at the lowest excitation power and room temperature).

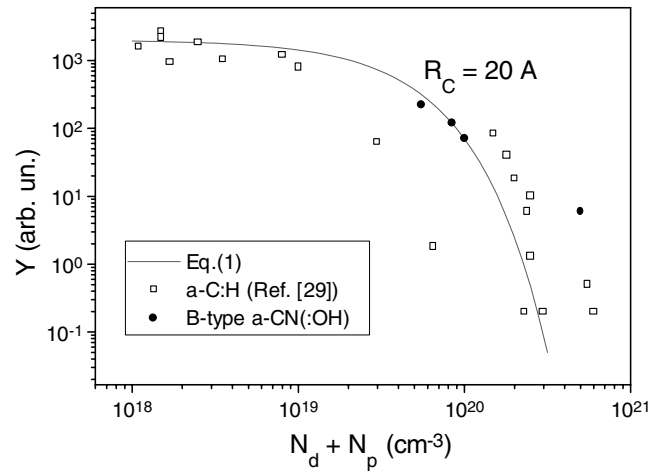


**Figure 7.** Plot of the PL efficiency versus total density of non-radiative centres. The continuous curve represents the fit of equation (1) with  $R_c = 20 \text{ \AA}$ .

The density of diamagnetic centres can be evaluated from the Gaussian density of ‘mixed’ ( $\pi + \text{LP}$ ) states  $N_{\pi+\text{LP}}(Z)$ , by estimating the total number of states at energy sitting below the threshold photon energy  $U$  at which PL and radiative recombination occur [29]:

$$N_d = \int_0^U N_{\pi+\text{LP}}(Z) dZ. \quad (4)$$

We observe that in the samples D0, . . . , D2 with low nitrogen content the optically active, diamagnetic centres ( $N_d \sim (5-10) \times 10^{19} \text{ cm}^{-3}$ ) forming bonding and antibonding states prevail on the paramagnetic centres ( $N_p \sim 10^{19} \text{ cm}^{-3}$ ), forming non-bonding states. Only in sample B, quite close to the transition to a C-type film (as suggested, for instance, by a little deviation from the Curie law below 8 K, and only weak presence of OH inclusions) we observe the prevalence of  $N_p > N_d$  ( $N_p \approx 4 \times 10^{20} \text{ cm}^{-3}$  and  $N_d \approx 1 \times 10^{20} \text{ cm}^{-3}$ ) resulting from optical and ESR measurements. Simultaneously, in this sample, the PL efficiency decreases

with power (i.e.  $\alpha < 0$ ) pointing at the increased importance of the Auger-like radiative recombination and corroborating the increased relevance of the non-bonding, paramagnetic recombination centres. However, also for this film, as for C-type films (see below) equation (1) does not hold.

#### 4.3. Recombination in 'C-type' a-CN

A different effect occurs in C-type a-CN thin films, always presenting  $\alpha < 0$  (figure 6, right axis). Indeed, in such films equation (1) (which has proved to be valid, with proper modifications, for B-type a-CN and a-C:H) no longer holds (see figure 7). It should be stressed that it is not only a matter of a different size  $R_C$  featuring the non-radiative centres in C-type a-CN. Indeed, in the case of samples exhibiting Pauli paramagnetism, we will have extended paramagnetic states and  $R_C$  tends to infinity. However, it can be observed that a residual luminescence occurs, while equation (1) would indicate  $Y = 0$ . This is still an open problem. A possible hypothesis is that in amorphous carbon-based materials the 'Auger' contribution to the PL efficiency (which in most PL materials is usually weak) must be added to that given by equation (1), assuming such an equation to describe the 'defects' as always involving non-radiative processes.

### 5. Conclusions

In conclusion, we have discussed the effects quenching the PL in carbon nitride-based thin films. The differentiation of reactively sputtered carbon nitride thin films in two different categories [20] depending on their infrared, structural and paramagnetic properties has been proved to be able to also describe their PL properties. In floppier, 'bubbly' (B-type) a-CN thin films, with higher gaps and semiconducting behaviour, the photoluminescent recombination of the light-induced electron-hole pairs takes place both via geminate and non-geminate processes. The non-radiative recombination processes can be described in terms of the same models as have been developed for non-nitrogenated, polymer-like amorphous carbons (a-C:H). Such processes are due to 'defect' states sitting close to the Fermi level, either diamagnetic or paramagnetic. The importance of the paramagnetic recombination centres on the overall PL recombination processes increases when the spin density increases but the optical gap remains quite large. In more compact a-CN thin films the PL is much lower but, despite the extended nature of high numbers of defects, a residual luminescence, attributed to 'Auger'-like radiative processes involving the defect states, is observed.

### References

- [1] Robertson J 1997 *Diamond Relat. Mater.* **6** 212
- [2] Kaufman J H, Metin S and Saperstein D D 1989 *Phys. Rev. B* **39** 13053
- [3] Muhl S and Mendez J M 1999 *Diamond Relat. Mater.* **8** 1809
- [4] Fanchini G, Tagliaferro A, Messina G, Santangelo S, Paoletti A and Tucciarone A 2002 *J. Appl. Phys.* **91** 1155
- [5] Fanchini G, Ray S C, Tagliaferro A and Laurenti E 2002 *Diamond Relat. Mater.* **11** 1143
- [6] Mutsukura N and Achita K 1999 *Diamond Relat. Mater.* **8** 1720
- [7] Riedel R 1998 *Chem. Mater.* **10** 2964
- [8] Victoria N M, Hammer P, DosSantos M C and Alvarez F 2000 *Phys. Rev. B* **61** 1083
- [9] Silva S R P, Robertson J, Amaratunga G A J, Rafferty B, Brown L M, Schwan J, Franceschini D F and Mariotto G 1997 *J. Appl. Phys.* **81** 2626
- [10] McKenzie D R, Li W T, Gerstner E G, Merchant A, McCulloch D G, Marks N and Bilek M M 2001 *Diamond Relat. Mater.* **10** 230
- [11] Dasgupta D, Demichelis F, Pirri C F and Tagliaferro A 1991 *Phys. Rev. B* **43** 2131

- [12] Fanchini G, Ray S C and Tagliaferro A 2002 *Surf. Coat. Technol.* **151/152** 233
- [13] Liu Y C, Demichelis F and Tagliaferro A 1996 *Solid State Commun.* **100** 597
- [14] Godet C, Heitz T, Bouree J E, Bouchet B, Dixmier J and Drevillon B 1999 *Solid State Commun.* **111** 293
- [15] Zhang M, Nakayama Y and Kume M 1999 *Solid State Commun.* **110** 679
- [16] Demichelis F, Rong X, Schreiter S, Tagliaferro A and DeMartino C 1995 *Diamond Relat. Mater.* **4** 361
- [17] Lejeune M, Durand-Drouhin O, Zellama K and Benlahsen M 2001 *Solid State Commun.* **120** 337
- [18] Demichelis F, Kaniadakis G, Tagliaferro A and Tresso E 1987 *Appl. Opt.* **26** 1737
- [19] Stief R, Schaefer J, Ristein J, Ley L and Beyer W 1996 *J. Non-Cryst. Solids* **198–200** 636
- [20] Fanchini G, Messina G, Paoletti A, Ray S C, Santangelo S, Tagliaferro A and Tucciarone A 2002 *Surf. Coat. Technol.* **151/152** 257
- [21] Fanchini G, Ray S C and Tagliaferro A *Solid State Commun.* submitted
- [22] Ottaviani G, 2001 private communication
- [23] Colthup N B, Daly L and Wiberley S E 1990 *Introduction to Infrared Spectroscopy* (Boston, MA: Academic)
- [24] Sokrates G 1980 *Infrared Characteristic Group Frequencies* (Chichester: Wiley)
- [25] Lacerda M M, Freire F L Jr and Mariotto G 1998 *Diamond Relat. Mater.* **7** 412
- [26] Iwasaki T, Aono M, Nitta S, Habuchi H, Itoh T and Nonomura S 1999 *Diamond Relat. Mater.* **8** 440
- [27] Robertson J 1995 *Diamond Relat. Mater.* **4** 297
- [28] Silva S R P, Robertson J, Rusli E, Amaratunga G A J and Schwan J 1996 *Phil. Mag. B* **74** 369
- [29] Giorgis F, Giuliani F, Pirri C F, Tagliaferro A and Tresso E 1998 *Appl. Phys. Lett.* **72** 2520
- [30] Street R A 1981 *Phys. Rev. B* **23** 861
- [31] von Bardeleben H J, Cantin J L, Zeinert A and Zellama K 2001 *Appl. Phys. Lett.* **78** 2843
- [32] Fanchini G, Tagliaferro A, Dasgupta D, Laurenti E, Ferrari A C, Milne W I and Robertson J 2002 *J. Non-Cryst. Solids* **299–302** 840
- [33] Street R A 1980 *Phys. Rev. B* **21** 5775